Antibody Therapeutics, 2024, Vol. 7, No. 1 77–87
https://doi.org/10.1093/abt/tbad032
Advance Access Publication on 5 January 2024

Research Article

GB12-09, a bispecific antibody targeting IL4Rα and IL31Rα for atopic dermatitis therapy

Feiyan Deng[1], Yuxin Qiu[1], Xiangling Zhang[1], Nining Guo[1], Junhong Hu[1], Wenjie Yang[1], Wei Shang[1], Bicheng Liu[2] and Suofu Qin[1,*]

[1]Drug Discovery, Center for Research and Development, Kexing BioPharma Co., Ltd, Shenzhen 518057, China, and [2]Institute of Nephrology, Zhong Da Hospital, Southeast University School of Medicine, Nanjing 999077, China

Received: September 25, 2023; Revised: November 27, 2023; Accepted: December 18, 2023

ABSTRACT

Atopic dermatitis (AD) is a chronic inflammatory skin condition characterized by dysregulated immune responses. The key mediators of AD pathogenesis are T helper 2 (TH2) cells and TH2 cytokines. Targeting interleukin 4 (IL4), IL13 or IL31 has become a pivotal focus in both research and clinical treatments for AD. However, the need remains pressing for the development of a more effective and safer therapy, as the current approaches often yield low response rates and adverse effects. In response to this challenge, we have engineered a immunoglobulin G—single-chain fragment variable (scFv) format bispecific antibody (Ab) designed to concurrently target IL4R and IL31R. Our innovative design involved sequence optimization of VL-VH and the introduction of disulfide bond (VH44-VL100) within the IL31Rα Ab scFv region to stabilize the scFv structure. Our bispecific Ab efficiently inhibited the IL4/IL13/IL31 signaling pathways *in vitro* and reduced serum immunoglobulin E and IL31 levels *in vivo*. Consequently, this intervention led to improved inflammation profiles and notable amelioration of AD symptoms. This research highlighted a novel approach to AD therapy by employing bispecific Ab targeting IL4Rα and IL31Rα with potent efficacy.

Statement of Significance: This research highlighted a novel approach to atopic dermatitis therapy by employing bispecific antibody targeting IL4Rα and IL31Rα with potent efficacy.

KEYWORDS: atopic dermatitis; bispecific antibody; TH2 cytokines; IL4Rα; IL31Rα

INTRODUCTION

Atopic dermatitis (AD), a chronic, lifelong and recurrent inflammatory skin disorder, presents a clinical spectrum encompassing xerosis, erythema, oozing, edema, crusting, lichenification, dyspigmentation, excoriation and more [1]. The condition affects an estimated 10% of adults and 25% of adolescents [2]. Notably, 20–46% of adult AD patients experience moderate to severe symptoms, imposing substantial physiological, psychological and economic burdens. Different symptoms manifest at various stages, but persistent pruritus remains a hallmark across nearly all phases, significantly impacting patients' quality of life and disease progression.

The pathophysiology of AD is intricate, involving a wide array of factors, including genetic, environmental, neurological, immune and microbiological components. Epidermal dysfunction and T-cell-driven inflammation constitute the principal mechanisms underpinning AD [2, 3]. Particularly, the T helper 2 (TH2) immune response plays a pivotal role in AD development. Elevated serum levels of TH2 cytokines, such as interleukin 4 (IL4), IL13 and IL31, have been detected in AD patients in comparison to healthy individuals. These findings correlate with heightened total serum immunoglobulin E (IgE) and circulating eosinophils [4–8]. In addition, IL4 and IL13 are strong suppressors of Filaggrin expression [9], and the high expression of IL4/IL13 aggravates the dry skin and skin barrier dysfunction [4]. Thymic stromal lymphopoietin and TH2-derived IL31 stimulate sensory neurons causing pruritus and subsequent scratching, which further

*To whom correspondence should be addressed. Suofu Qin, Drug Discovery, Center for Research and Development, Kexing BioPharma Co., Ltd, Shenzhen 518057, China. Email: qinsuofu@hotmail.com

worsens skin barrier disruption. IL31 also binds to the receptors on the surface of immune cells and keratinocytes, releasing chemokines that recruit inflammatory cells and exacerbating the inflammatory response [4].

Dupilumab, a monoclonal antibody (Ab) that blocks IL4Rα and hinders IL4 and IL13 effects, has gained global recognition as an effective treatment for moderate-to-severe AD [10–12]. Tralokinumab, an Ab for blocking IL13, has been approved for treatment of AD [13–15]. Nemolizumab, a humanized Ab against IL31Rα and blocking IL31 signaling pathway, has been approved in Japan for use in adults and children over the age of 13 for the treatment of itch associated with AD [16]. In clinical treatments for patients with moderate-to-serve AD, Dupilumab, Tralokinumab and Nemolizumab partly improve the symptoms of AD, including eczema, pruritus and so on. Nonetheless, clinical treatments involving Dupilumab or Nemolizumab alone reveal certain shortcomings, including limited overall effectiveness, suboptimal relief from itching and the occurrence of side effects [10–12, 16–18]. It is essential for depth research in developing a new and effective therapy for patients with AD.

Bispecific antibodies (Abs), a large family of molecules designed to recognize two different epitopes or antigens simultaneously, come in over 100 different formats, ranging from relatively small single-chain molecules, merely consisting of two linked Ab fragments, to large immunoglobulin G (IgG)-like molecules and large complex molecules with additional domains attached [19, 20]. Compared with monospecific Ab, bispecific Ab shows its superiority of effectively preventing drug resistance, targeting dual immune checkpoints to enhance efficacy or novel functionalities [19]. Over the past decades, a great number of bispecific Abs are in clinical development, some of which have been approved as drugs, including catumaxomab for the intraperitoneal treatment of malignant ascites [21], blinatumomab for the treatment of B-cell malignancies [22] and emicizumab for the treatment of hemophilia A [23]. In this research, we attempted to find a novel treatment modality for AD by screening out a drug-able bispecific Ab from different formats, targeting IL4Rα and IL31Rα, and successfully blocking IL4/IL13/IL31. It might combine the blocking efficacy of TH2-type cytokines-related inflammatory pathways in skin immune microenvironment and IL31-related signal transduction pathway in sensory neurons, leading to greater efficacy for AD therapy and better patient compliance.

This study demonstrates the development and characterization of a novel bispecific Ab GB12-09, capable of targeting both IL4Rα and IL31Rα. This bispecific Ab effectively disrupts IL4/IL13-IL4Rα and IL31-IL31Rα signaling pathways in both *in vitro* and *in vivo* settings, exhibiting heightened efficacy in suppressing TH2/TH2 cytokines associated with AD.

MATERIALS AND METHODS

Cell line and reagents

IL4/IL13 reporter 293 cell line was purchased from Genomeditech (GM-C01511). BaF3 cell line was obtained from BNCC (BNCC339311) and hIL31Rα/hOSMR BaF3 cell line was created by transfecting hIL31Rα and hOSMR into BaF3 cell through lentiviral vector. hIL4Rα-Fc (10402-H02H), hIL31Rα-Fc (15878-H02H), hIL31Rα-His (15878-H08H), hIL31 (11557-H08H) and mIL3 (51066-MNAH) were from Sino Biological; hIL4Rα-His (LR-M52H1) and hIL4 (IL4-H4218) were from Acro; hIL13 (CC89) was from Novoprotein; HRP anti-His (ab1187) was purchased from Abcam. One-Lite™ Luciferase Assay System was obtained from Vazyme (DD1203-01). CellTiter-Glo® Luminescent Cell Viability Assay was manufactured by Promega (G7572).

Ab generation, expression and purification

GB12-09 was a tetravalent bispecific, humanized IgG_4 Ab targeting hIL4Rα and hIL31Rα, whereas GB12-40 targeting hIL4Rα and mIL31Rα. The two composing Abs of GB12-09, namely, anti-hIL4Rα and anti-hIL31Rα, were sourced from Dupilumab and Nemolizumab. hIL31Rα (GB12-09) or mIL31Rα (GB12-40) Ab single-chain Fv (scFv) module was added to the C-terminus of the heavy chains of full IL4Rα Ab using a $(G_4S)_4$ connector based upon the tetravalent 'Morrison format' [24]. A VH44-VL100 (Kabat numbering) disulfide bond was introduced in the anti-IL31Rα scFv linking to the C-terminus in GB12-09 and GB12-40.

Two plasmids encoding the heavy and light chain, respectively, were transient transfected into HEK293-F (Invitrogen, A14527CN) according to the manufacturer's instruction. The supernatant was harvested after 7 days and Abs were purified from the supernatant using a Protein A Sepharose column (Sino Biological, 10600-P07E-RN).

Determination of the Ab's purity by size exclusion chromatography

The BioCore SEC-300 (NanoChrom, China) with a mobile phase of phosphate buffer solution in Milli-Q water at a flow rate of 0.5 mL/min was used to analyze our Abs. The temperature of column was 30°C. The total collection time was 35 min. The samples were diluted to 1 mg/mL with mobile phase, and then were centrifuged at 9710 × *g* for 10 min at 4°C. In all, 50 μL of each sample was injected. Ultraviolet (UV) absorption at 280 nm was used to monitor the elution.

Determination of the Ab's purity by capillary electrophoresis with sodium dodecyl sulfate under nonreducing condition

Overall, 100 μg of sample and 5 μL 0.25 M 2-Iodoacetamide were mixed in a 1.5 mL centrifuge tube, and the final concentration of sample was 1 mg/mL diluted in sodium dodecyl sulfate buffer. The sample was incubated at 70°C for 10 min, cooled at room temperature for 3 min at least, vortexed, centrifuged at 6000 × *g* for 1 min at 25°C, and 90 μL supernatant was transferred into a micro sample tube. Capillary electrophoresis with sodium dodecyl sulfate (CE-SDS) separations were performed on ProteomeLab PA 800 plus system (AB Sciex, Redwood City, CA) using a

30.2 cm bare fused silica capillary. The effective separation length was 20 cm. Samples were introduced into the capillary by electrokinetic injection in reverse polarity at 5 kV for 20 s. Separation was achieved by applying 15 kV for 35 min. UV detection of migrating proteins was monitored at 220 nm.

Bio-layer interferometry

The affinity between Ab and receptor was assessed using the Octet® R8 Bio-layer Interferometry (BLI) system from Sartorius. This analysis was conducted in PBS at pH 7.4, supplemented with 0.1% BSA and 0.02% Tween, at a temperature of 25 °C. GB12-09 or GB12-40 was immobilized onto ProA biosensors (Sartorius, 18-5010) until a BLI signal response of 1 nm was achieved. To measure association rates, the loaded biosensors were transferred to wells containing a 2-fold serially diluted hIL31Rα-His or mIL31Rα-His, ranging from 100 to 1.56 nM. Dissociation rates were determined by dipping the biosensors into buffer-containing wells. The association duration was set at 180 s, followed by a dissociation period of 400 s.

Hydrophobic interaction chromatography

Abs' solubility index was detected indirectly using a hydrophobic interaction chromatography (HIC) assay. The optimized HIC method was performed with a Protemix HIC Butyl-NP5 column (4.6 × 100 mm, 5 μm; Sepax). Mobile phase A consisted of 0.1 M sodium dihydrogen phosphate, 1.8 M ammonium sulfate, pH 6.5; mobile phase B was 0.1 M sodium dihydrogen phosphate, pH 6.5. The column temperature was maintained at 25°C and the sample temperature was maintained at 8°C. The flow rate was 1.0 mL/min with a gradient from 44 to 100% B in 20 min, followed by a 5 min isocratic hold with 44% B at the end of the gradient to ensure complete elution.

Differential scanning fluorimetry

A differential scanning fluorimetry (DSF) assay was performed using a Nano DSF system (Pronetheus NT48). Briefly, 20 μL of Ab solution was loaded into the capillaries. The samples were heated from 20 to 90°C at a rate of 1°C/min, and fluorescence signals were collected and analyzed.

Dual-target bridging ELISA

The method was referred to the protocol by Min Pei [25]. A 96-well microplate was coated with 100 μL of 2 μg/mL IL31Rα-Fc protein per well, covered with a lid and incubated at 4°C for overnight. The next day, the coating solution was removed. The coated microplate was washed three times with 200 μL of PBS per well, blocked with 100 μL of 2% BSA in PBS buffer per well and incubated for 2 h at 37°C. Then the blocking solution was discarded and the microplate was washed three times with 200 μL PBST per well. Stock solution of 200 nM GB12-09/anti-hIL4Rα/anti-hIL31Rα was 4-fold serially diluted in PBS buffer. In all, 100 μL of each diluted Ab was added in triplicates and incubated for 2 h at 37°C. Next, the microplate was washed three times with 200 μL PBST per well. Overall, 50 μL of 24 nM hIL4Rα-His in PBS buffer was added into each well, and incubated for 2 h at 37°C. Next, the microplate was washed with 200 μL PBST per well three times. In all, 50 μL of pre-prepared HRP anti-His Ab (1:5000) in PBS buffer was pipetted into each well, incubated for 1 h at 37°C and discarded. Microplate was washed with 200 μL PBST per well six times. Color was developed by adding 50 μL of TMB substrate solution to each well for 3–15 min at room temperature, stopped with 50 μL of 2 M sulfuric acid per well and measured at OD450 using a microplate reader. In addition, hIL4Rα-Fc (1 μg/mL) was used to capture Ab and then detected with hIL31Rα-His.

Reporter gene assay

IL4/IL13 reporter 293 cell line was cultured in DMEM medium with 10% FBS, 1% penicillin–streptomycin, 0.75 μg/mL puromycin and 4 μg/mL blasticidin. In all, 20 000 cells in 50 μL assay medium were seeded per well in 96-well microplate one day in advance. GB12-09, anti-hIL4Rα and anti-hIL31Rα were serially diluted at a ratio of 1:2 in the assay medium (DMEM with 1% FBS) at a starting concentration of 40 nM, respectively. IL4 was diluted to 2 ng/mL in assay medium. Then, the cultured medium was replaced by adding 50 μL of the serial Ab diluents and 50 μL of the diluted IL4 solution to each well. After 6-h incubation at 37°C with 5% CO_2, 100 μL of One-Lite™ Luciferase Assay System solution was added to each well, and the microplate was shaken for 2 min using a titer plate shaker and stood at room temperature for 13 min. Relative luciferase units (RLUs) were later measured using a microplate reader. For the detection of IL13 blocking activity, Abs were gradient-diluted at a starting concentration of 20 nM in the assay medium (DMEM with 1% FBS). Cells were incubated for 6 h with 20 ng/mL IL13 and gradient-diluted Abs.

IL31-dependent BaF3 cell proliferation assay

hIL31Rα/hOSMR BaF3 cell was cultured in RPMI1640 medium with 10% FBS, 10 ng/mL rmIL3, 1.2 μg/mL puromycin and 28 μg/mL blasticidin. hIL31Rα/hOSMR BaF3 cell was centrifuged and washed with PBS three times. In all, 10 000 cells in 50 μL assay medium (RPMI 1640 with 10% FBS) per well were seeded in 96-well microplate. GB12-09, anti-hIL4Rα and anti-hIL31Rα were serially diluted at a ratio of 1:3 in the assay medium (RPMI 1640 with 10% FBS) at a starting concentration of 100 nM, respectively. hIL31 was diluted to 4 ng/mL in assay medium. Then, 25 μL of the serial Ab diluents and 25 μL of the diluted IL31 solution were added to each well. After 48-h incubation at 37°C with 5% CO_2, 50 μL of CellTiter-Glo® Luminescent Cell Viability Assay solution was added to each well, and the microplate was shaken for 2 min using a titer plate shaker and stood at room temperature for 10 min. Luminescence was later measured using a microplate reader.

Animal and DNFB sensitization

Six-weeks-old male hIL4/hIL4Rα BALB/c mice from Biocytogen (111889, China) were used to verify the efficacy of our bispecific Ab. The hairs of the same area in the back were removed from anesthetized mice using an electric shaver at 1 week after arriving (Day 0). The next day (Day 1), the mice were weighed and the right ear thickness of each mouse was measured. Both sides of the right ear and the exposed skin in the back of mice in blank group (eight mice) were treated with 25 μL solvent (a 4:1 mixture of acetone and olive oil), whereas the others were treated with 25 μL of 0.5% DNFB in solvent. The thickness of right ear of mice was measured and DNFB-treated mice were divided into five groups with the same mean thickness of ear on Day 3 and the second challenge with 0.2% DNFB happened on Day 5. The specific group information was shown in Fig. 5B. On Day 4/7/11, mice were treated with equal volumes of PBS, anti-hIL4Rα, anti-mIL31Rα, combo of anti-hIL4Rα and anti-mIL31Rα or GB12-40 by intraperitoneal injections. On Day 13, mice were scarified and the blood samples were harvested. Ear thicknesses of mice were assessed on Day 3/5/7/9 by using a vernier caliper.

Measurement of serum cytokines

Serum samples were separated from the blood collected on Day 13 and stored at −20°C until analyzed. Levels of total serum IgE and IL31 were measured using ELISAs (Thermo, 88-50460-88; Thermo, BMS6030TEN) according to the instructions of the manufacturer.

Statistical analysis

All data were expressed as the mean ± standard deviation. Statistical analysis was performed by one-way analysis of variance using GraphPad Prism 8 Software. $P < 0.05$ was considered as statistically significance. The significance levels of the data were denoted as $^{*}P < 0.05$, $^{**}P < 0.01$, $^{***}P < 0.001$.

RESULTS

Designing and expressing GB12-09, a bispecific Ab

Because of the key role of the TH2 cells and TH2 cytokines in the development of AD, we selected IL4Rα and IL31Rα as the targets to build a bispecific Ab. Symmetric formats are more similar to native Abs, and more friendly to industrial production. Fc-retained formats have a relatively longer plasma half-life, beneficial to clinical development. Therefore, symmetric Fc-retained format was preferred. Over 60 bispecific Ab molecules were designed, based on an anti-hIL4Rα monospecific Ab and an anti-hIL31Rα monospecific Ab. The main design strategies were shown in Fig. 1A, involving multiple combinations of the following adjustments: different antigen-binding site fragment formats, adjustment of the order of VH/VL in the fused scFv, introduction of disulfide bond in the fused scFv, different linking sites of the fused scFv, selection of different IgG subclasses and so on. Purity and impurity were evaluated and analyzed with nonreduced CE-SDS (nrCE-SDS) and size exclusion chromatography (SEC). Among the Abs analyzed, we identified a bispecific Ab GB12-09 with the purity of SEC 95.9% and nrCE-SDS 93.91% as shown in Fig. 1C and D. The format of GB12-09 was shown in Fig. 1B. It retained the whole anti-hIL4R Ab, linking with the anti-hIL31R-scFv at the C-terminus of heavy chain.

We conducted a comprehensive assessment of critical properties for GB12-09, including solubility index and thermal stability. The solubility index was indirectly determined using a HIC assay, with detailed results provided in Table S1. Notably, the retention time of GB12-09 in the column exceeded that of anti-hIL4Rα or anti-hIL31Rα, indicating a comparatively poorer solubility index than monospecific Abs. Furthermore, the thermal stability of GB12-09 was assessed using a DSF assay, revealing a melting temperature (T_{m1}) of 56.5°C (Table S2).

Effective *in vitro* targeting of IL4Rα and IL31Rα by GB12-09

We designed a bridging ELISA to detect if the bispecific Ab GB12-09 could specifically bind to the corresponding target at the same time. The results were shown in Fig. 2. When coating the microplate with hIL31Rα for capturing, GB12-09 specifically bound to the microplate and could be detected successfully by hIL4Rα-His binding on the other side of GB12-09 (Fig. 2A). In contrast, if coating the microplate with hIL4Rα, GB12-09 also could bind to the microplate and be detected successfully by hIL31Rα-His attaching to the other side of GB12-09 (Fig. 2B). The signal was enhanced with the increased concentration of GB12-09. Therefore, GB12-09 can bind to hIL31Rα and hIL4Rα at the same time.

Blocking IL4/IL13 and IL31 signaling pathways by GB12-09 *in vitro*

After verifying the binding activity of GB12-09 with both hIL31Rα and hIL4Rα, we wanted to know if they could block IL4Rα and IL31Rα signaling pathways in cells. First, we detected the IL4Rα signaling pathway activity through a reporter gene assay with IL4/IL13 reporter 293 cell line, where IL4Rα was the common receptor subunit of IL4 and IL13. The results showed that GB12-09 blocked the hIL4 (Fig. 3A) and hIL13 (Fig. 3B) activity successfully. The inhibition of hIL4/hIL13 activity by GB12-09 was similar to that by anti-hIL4Rα monospecific Ab. The blocking of IL31Rα signaling activity was detected with a hIL31Rα/hOSMR stable expression cell line whose proliferation was hIL31-dependent. As the result shown in Fig. 3C, GB12-09 decreased the hIL31-dependent cell proliferation and blocked IL31-IL31R signaling activity.

Preventing IL4/IL13 signaling pathway *in vitro* by GB12-40, a modified version of GB12-09 by replacing the hIL31R Ab's scFv with mIL31R Ab's scFv

The *in vivo* hIL4Rα inhibition efficacy of our bispecific Ab could be carried out in hIL4/hIL4Rα mice. However, the hIL31R inhibition efficacy could not be evaluated

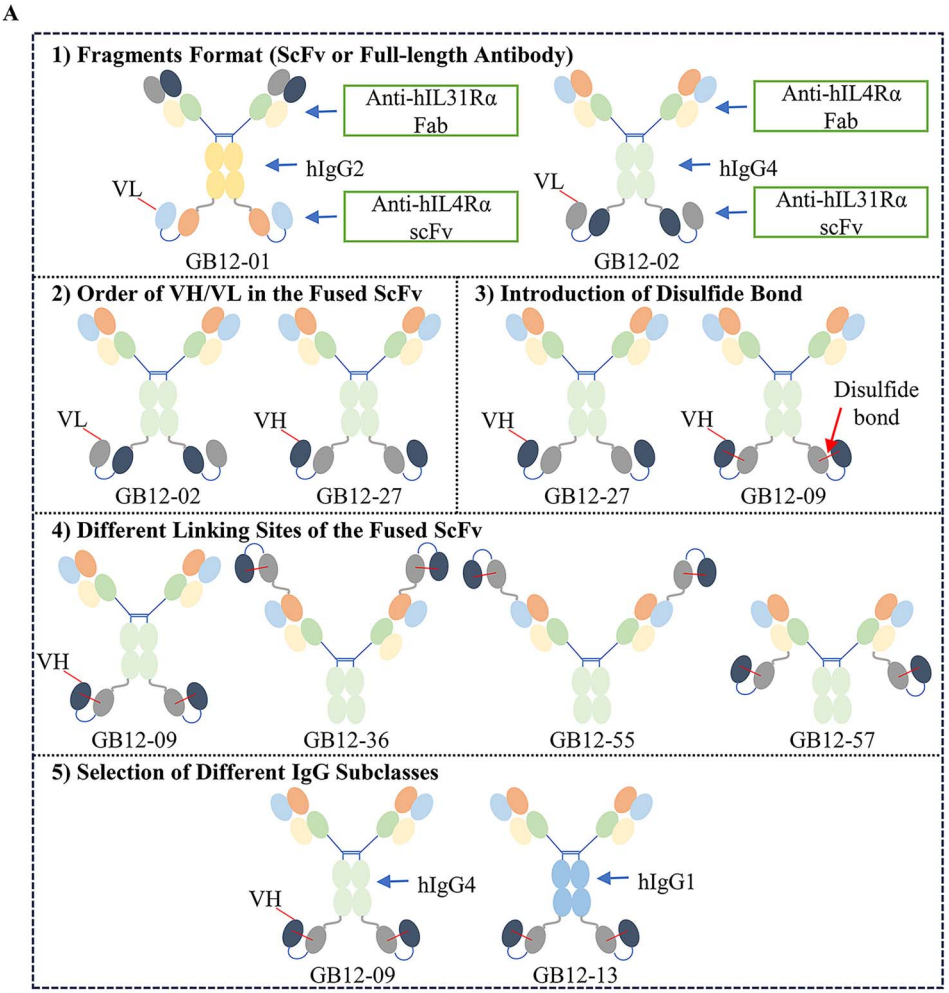

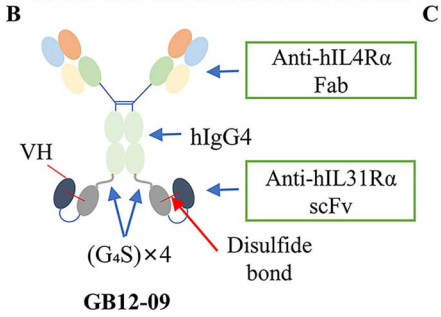

C

Molecular Number	SEC	nrCE-SDS
GB12-01	58.30%	92.30%
GB12-02	30.90%	65.92%
GB12-09	95.90%	93.91%
GB12-13	97.26%	97.10%
GB12-27	87.00%	96.02%
GB12-36	87.92%	89.31%
GB12-55	77.95%	83.75%
GB12-57	74.49 %	67.78 %

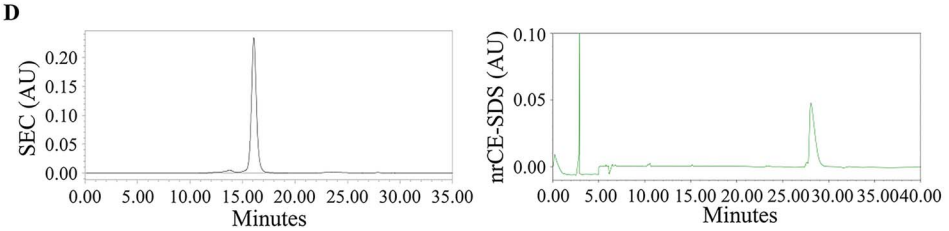

Figure 1. Structures of bispecific Abs and the purity of GB12-09. (A) The specific adjustments in format of designed bispecific Abs. (B) The format of GB12-09. (C) Purity of molecules by SEC and nrCE-SDS. The purity was determined through SEC and nrCE-SDS analysis. The BioCore SEC-300 (NanoChrom, China) with a mobile phase of phosphate buffer solution in Milli-Q water at a flow rate of 0.5 mL/min was used to analyze Abs. NrCE-SDS separations were performed on ProteomeLab PA 800 plus system (AB Sciex, Redwood City, CA) using a 30.2 cm bare fused silica capillary. (D) Chromatograms of GB12-09 by SEC (left) and nrCE-SDS (right).

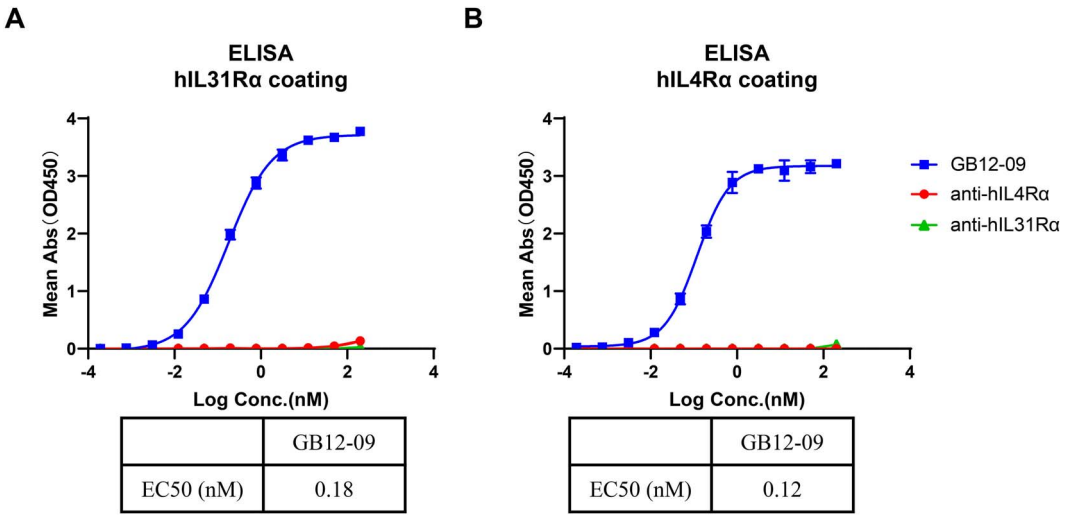

	GB12-09
EC50 (nM)	0.18

	GB12-09
EC50 (nM)	0.12

Figure 2. GB12-09 successfully targeted IL4Rα and IL31Rα simultaneously *in vitro*. The dual-target bridging ELISA was used to evaluate whether GB12-09 bound to hIL4Rα and hIL31Rα simultaneously. Whether utilizing hIL31Rα-Fc (A) or hIL4Rα-Fc (B) recombinant proteins to capture GB12-09, the signal could be detected consistently by assessing the His Tag of hIL4Rα-His (A) or hIL31Rα-His (B), which bound to the other side of GB12-09. Data analysis was performed using GraphPad.

because of no cross activity. For this reason, anti-hIL31R scFv sequence was replaced with an anti-mIL31Rα scFv in GB12-09, which created the GB12-40 (Fig. 4A). The affinity of GB12-40/mIL3Rα (6.92 nM) was found to be comparable to that of GB12-09/hIL31Rα (8.97 nM) (Fig. 4A). The result in Fig. 4B showed that GB12-40 still inhibited the IL4 and IL13 signaling pathway activity in the same way as anti-hIL4Rα monospecific Ab. This change had no effect on the anti-hIL4Rα activity of bispecific Ab.

Relieving the inflammatory responses in DNFB induced murine AD model by GB12-40

An AD-like murine model induced by DNFB was established for *in vivo* study as the experimental schedule in Fig. 5A and group information was shown in Fig. 5B. Mice were sensitized with 0.5% DNFB on Day 1 and rechallenged with 0.2% DNFB on Day 5. The results in Fig. 5C showed that ear thickness of mice in DNFB treated groups increased while those in group vehicle kept still, meaning the ear inflammation of mice in groups treated with DNFB. Compared with PBS or anti-hIL4Rα or anti-mIL31Rα alone, combo (anti-hIL4Rα + anti-mIL31Rα) or GB12-40 significantly suppressed the continuous thickening ears in DNFB-induced AD-like mice on Day 9 after the second Ab treatment.

Activated TH2 cells secrete IL4 and IL13 which promote the production of IgE, leading to the AD. The serum total IgE of each group was assayed and the result was shown in Fig. 5D. Compared with PBS, treatment of anti-hIL4Rα monospecific Ab, GB12-40 alone or combo (anti-hIL4Rα + anti-mIL31Rα) obviously decreased the serum total IgE level in DNFB-induced AD-like mice, whereas treatment of anti-mIL31Rα alone had no effect. In comparison, the serum IL31 was only declined clearly in DNFB-induced AD-like mice treated with combo or GB12-40 (Fig. 5E).

DISCUSSION

AD is a chronic, relapsing, inflammatory skin disease with a lifetime prevalence of up to 20%, which has serious effect on quality of life [26]. In this research, we demonstrated a novel treatment modality for AD by a bispecific Ab targeting IL4Rα and IL31Rα and then blocking IL4/IL13/IL31 signaling pathways. We have constructed over 60 bispecific Abs in this study. The key point of our design strategies was the symmetric Fc-retained format for keeping the basal stability and quality, then adjustments were made in formats according to the results of SEC and nrCE-SDS, which were widely used for purity evaluation and impurity analysis of Abs, and the aggregation and fragment issues were reflected in the detection results [27]. The main formats were shown in Fig. 1A. According to the SEC/nrCE-SDS results (Fig. 1C), GB12-27 showed higher purity of SEC and nrCE-SDS than GB12-02. Fusing the scFv with the whole Ab in the order of VH-linker-VL-C-terminus of heavy chain increased both SEC and nrCE-SDS purity of molecule, whereas aggregation and fragment issues were circumvented. It has been shown that a C-terminal heavy chain-attached scFv construct stabilized by a VH44-VL100 disulfide bond was identified as the most optimal molecule with properties similar to those of conventional Abs, based on the high production yield and low aggregation tendency [28–33]. To further stabilize the scFv and prevent aggregation, we induced a VH44-VL100 disulfide bond in the anti-IL31Rα scFv by mutating both G to C in VH44 and VL100, respectively, and then GB12-09 was created. Compared with GB12-27, GB12-09 was more stable with the presence of extra disulfide bond and the SEC purity increased (from 87 to 95.9%), suggesting a lower tendency of aggregation and reduced self-interaction.

Next, we evaluated the binding activity and whether GB12-09 was biological active *in vitro* and *in vivo*. Through a dual-target bridging ELISA, we found that GB12-09

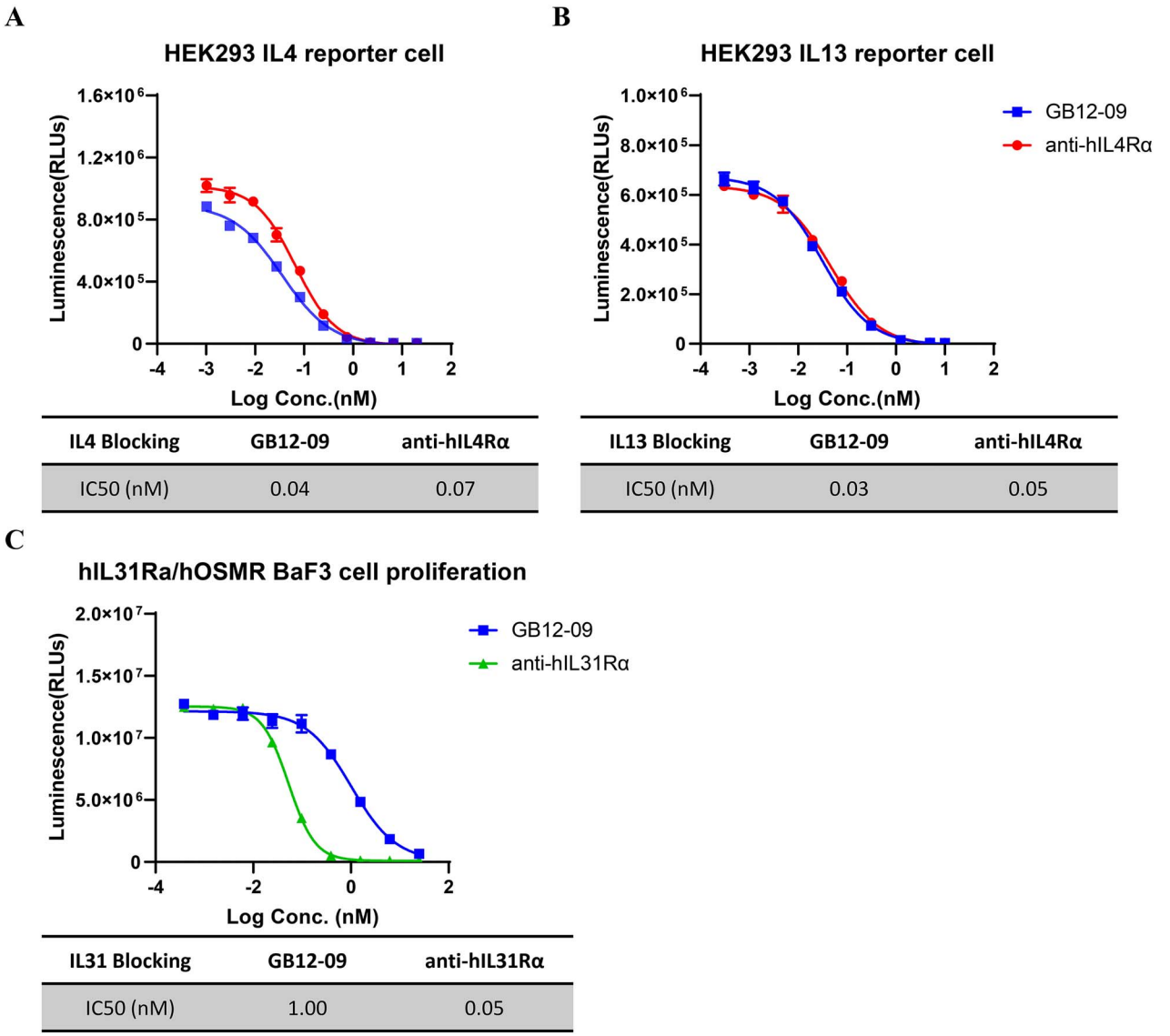

IL4 Blocking	GB12-09	anti-hIL4Rα
IC50 (nM)	0.04	0.07

IL13 Blocking	GB12-09	anti-hIL4Rα
IC50 (nM)	0.03	0.05

IL31 Blocking	GB12-09	anti-hIL31Rα
IC50 (nM)	1.00	0.05

Figure 3. GB12-09 effectively blocked the IL4, IL13 and IL31 signaling pathways *in vitro*. (A, B) GB12-09/anti-hIL4Rα exhibited a reduction in IL4 and IL13 activity. IL4/IL13 reporter 293 cells were seeded at a density of 20 000 cells per well in a 96-well microplate, activated with hIL4 at a final concentration of 1 ng/mL (A) or 20 ng/mL hIL13 (B) and then incubated with serial Ab concentrations for 6 h. RLUs were subsequently measured. (C) GB12-09/anti-hIL31Rα inhibited the hIL31-dependent BaF3 cell proliferation. hIL31Rα/hOSMR BaF3 cells were seeded at a density of 10 000 cells per well in a 96-well microplate, treated with hIL31 at a final concentration of 1 ng/mL and exposed to serial concentrations of Abs for 48 h. Cell viability was then assessed. Data analysis was performed using GraphPad.

binding with hIL4Rα did not affect its C-terminus binding to hIL31Rα, and it worked the other way around (Fig. 2). Inhibition of hIL4/hIL13-induced signaling by GB12-09 was comparable to that by anti-hIL4Rα in an IL4/IL13 reporter assay (Fig. 3A and 3B); however, prevention of hIL31-induced signaling was somewhat lower than that by anti-hIL31Rα in the hIL31-dependent hIL31Rα/hOSMR cell proliferation assay (Fig. 3C). It was likely associated with the anti-IL31Rα scFv structure in GB12-09 since the scFv module of hIL4Rα also had a partial loss of Ab activity once full-length hIL4Rα Ab was replaced (data not shown). Further research in format design is warranted for keeping the binding activity of two different epitopes or antigens. Regardless, we demonstrated that GB12-09 functionally blocked IL4/IL13/IL31 biological activity in deed *in vitro*. The dosage and frequency of dupilumab and Tralokinumab were both higher than Nemolizumab in clinical treatment [10–15, 17, 18], suggesting that less Ab was needed for blocking hIL31-hIL31Rα signaling pathway. Therefore, GB12-09 possibly showed the good hIL31Rα inhibition *in vivo* when the dosage of GB12-09 was similar to the monospecific hIL4Rα Abs just like Dupilumab or Tralokinumab. The structure of GB12-09 has achieved a good balance in blocking of hIL4Rα and hIL31Rα activity.

We then evaluated if GB12-09 could improve the symptoms of AD in the DNFB-induced murine AD model *in vivo*. IgE expression has positive correlation with

A

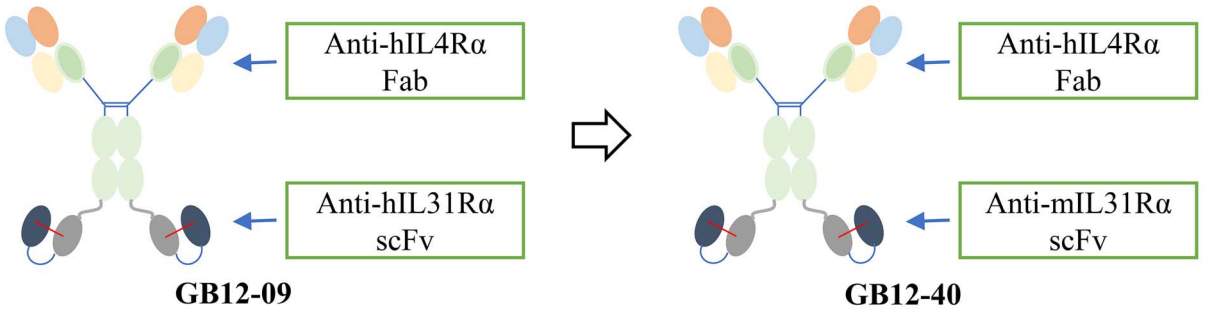

Molecular Number	GB12-09 (nM)	GB12-40(nM)
mIL31Ra Binding	/	6.92
hIL31Ra Binding	8.97	/

B

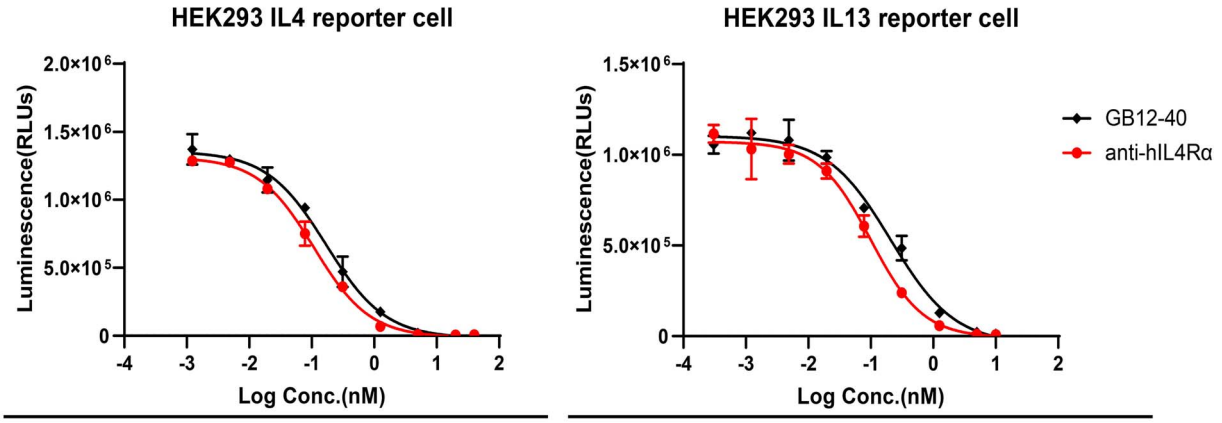

IL4 Blocking	GB12-40	anti-hIL4Rα
IC50 (nM)	0.17	0.11

IL13 Blocking	GB12-40	anti-hIL4Rα
IC50 (nM)	0.21	0.10

Figure 4. GB12-40 blocked the IL4/IL13 activity *in vitro*. (A) The structure of GB12-40. GB12-40, a substitute Ab of GB12-09, was developed by conjugating the scFv of the mIL31Rα Ab to the C-terminus of hIL4Rα Ab's heavy chain. The affinities of Abs with hIL31Rα or mIL31Rα were detected with a BLI system. (B) GB12-40 effectively maintained its ability to block IL4/IL13 activity *in vitro*. IL4/IL13 reporter 293 cells were seeded at a density of 20 000 cells per well in a 96-well microplate, activated with 1 ng/mL hIL4 or 20 ng/mL hIL13 and then incubated with serial concentrations of Abs for 6 h. RLUs were subsequently measured. Data analysis was performed using GraphPad.

IL4/IL13 protein level and the level of IgE is associated with the severity of AD [34–36]. In the DNFB-induced AD-like hIL4/hIL4Rα murine model, GB12-40, a substitute Ab of GB12-09 using anti-mIL31Rα scFv to replace the anti-hIL31Rα scFv (Fig. 4), reduced the total serum IgE level dramatically compared with PBS, whereas the IgE level was not affected via treating with anti-mIL31Rα only (Fig. 5D), demonstrating that our bispecific Ab GB12-40 successfully blocked IL4Rα signaling pathway *in vivo*. The ear thickness of mice is an inflammation index of ear skin [37]. The ear thickness was observed to be decreased in DNFB-induced AD-like mice after the second treatment of GB12-40 or Combo (anti-hIL4Rα and anti-mIL31Rα), compared with those treated with anti-hIL4Rα or anti-mIL31Rα only. This observation revealed that as effective as combo, GB12-40 reduced the inflammation in DNFB-induced AD-like murine model. As is well-known, IL31 is an itching-associated cytokines [38, 39]. Interestingly, serum IL31 level in AD-like mice was reduced by treatment with combo and GB12-40, but not by anti-hIL4Rα or anti-mIL31Rα only. It has been reported that IL31 expression is correlated with IL4 [40, 41]. However, it is still ambiguous about why the downregulation of IL31 expression requires both the IL4Rα and IL31Rα signaling pathway being blocked. It is speculated that blocking both IL4Rα and IL31Rα signaling pathway by the treatment of combo or GB12-40, relieves the inflammation to a great extent, reduces the itching and scratching, repairs the skin barrier and downregulates inflammatory cytokines expression including IL31, further improving the symptoms of AD.

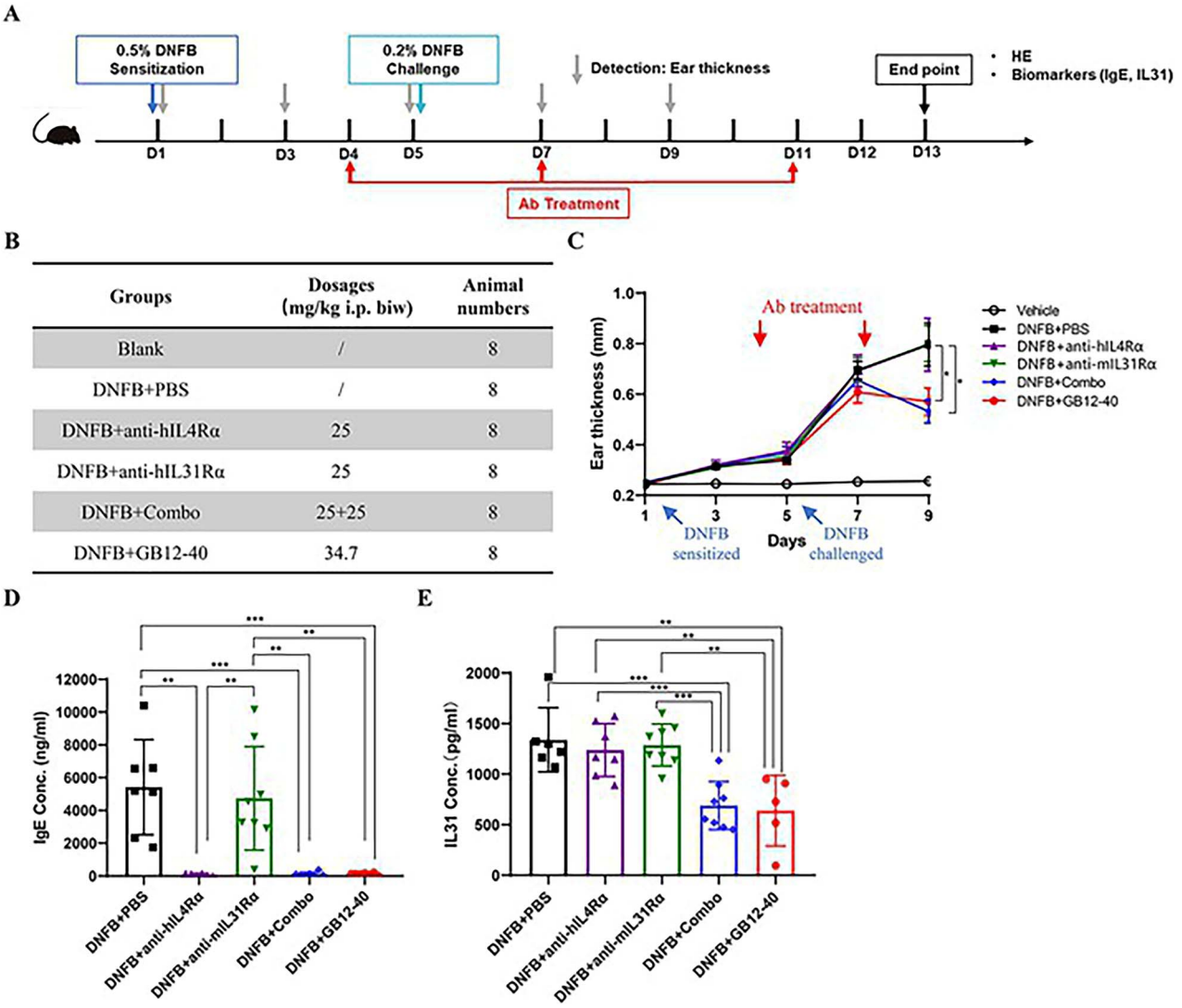

Groups	Dosages (mg/kg i.p. biw)	Animal numbers
Blank	/	8
DNFB+PBS	/	8
DNFB+anti-hIL4Rα	25	8
DNFB+anti-hIL31Rα	25	8
DNFB+Combo	25+25	8
DNFB+GB12-40	34.7	8

Figure 5. Assessing the *in vivo* efficacy of GB12-40 in a DNFB induced AD-like murine model. (A) Protocol overview: mice were initially sensitized with 0.5% DNFB on Day 1 and subsequently rechallenged with 0.2% DNFB on Day 5. On Days 4, 7 and 11, mice received intraperitoneal injections of equal volumes (with equal molarity) from different experimental groups. On Day 13, all mice were humanely euthanized, and blood samples were collected. (B) Groups information and molecular dosages. (C) Ear thickness measurement for each group. Ear thickness, an inflammation index of ear skin, was suppressed in GB12-40 or combo treated DNFB-induced AD-like mice, compared with PBS. DNFB + anti-hIL4Rα vs DNFB + GB12-40 (P-value = 0.0265), DNFB + anti-hIL4Rα vs DNFB + Combo (P-value = 0.0197). (D) Serum total IgE in each group. IgE expression is associated with the activation of IL4Rα signaling pathway and the level of IgE is associated with the severity of AD. Treatment of GB12-40, anti-hIL4Rα or combo reduced the serum level of IgE in DNFB-induced AD-like mice. (E) Serum total IL31 in each group. IL31, a cytokine closely related to itching, was downregulated in GB12-40 or combo treated DNFB-induced AD-like mice. Data analysis was performed using GraphPad.

In this study, we explored a novel treatment modality for AD using a bispecific Ab simultaneously targeting IL4Rα and IL31Rα. This dual targeting effectively blocked IL4/IL13/IL31 pathways. By combining the inhibition of TH2-type cytokines in the skin's immune microenvironment and IL31-related signal transduction pathway in sensory neurons, we anticipate enhanced efficacy, reduced side effects and improved patient compliance. First, we observed that IL4R was expressed in various tissues, whereas IL31R exhibited tissue-limited expression, particularly with higher levels in the skin (Fig. S1A and B, data from protein atlas, https://www.proteinatlas.org/). The bispecific Ab format may facilitate greater enrichment in skin tissue, potentially leading to increased efficacy. Despite similar *in vivo* efficacy between combination therapy and bispecific Ab, GB12-40 showed a better anti-inflammation efficacy than anti-IL4Rα or anti-IL31Rα alone. Second, while Dupilumab is a successful and well-tolerated therapy for AD, it is associated with common ocular adverse events such as conjunctivitis. Analysis of the protein atlas database revealed detectable IL4R in the eye, whereas IL31R expression was minimal (Fig. S1C and D, data from protein atlas, https://www.proteinatlas.org/). Utilizing a bispecific Ab format may potentially reduce Ab accumulation in the eyes, lowering the risk of ocular side effects. Third, treatment with bispecific Ab is

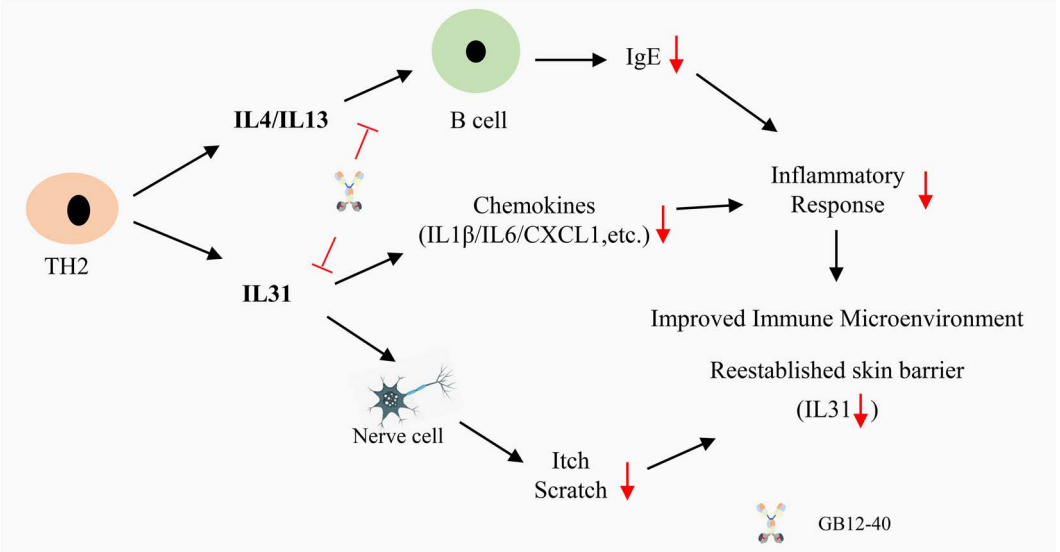

Figure 6. Schematic illustration of the mechanisms of action for IL4Rα/IL31Rα bispecific Ab in AD treatment. GB12-40, a bispecific Ab targeting IL4Rα and IL31Rα, effectively inhibits the IL4/IL13-IL4Rα and IL31-IL31Rα signaling pathways. Consequently, it reduces IgE and IL31 levels, alleviates the inflammatory response and mitigates AD symptoms.

more patient-friendly compared with combination therapy, significantly improving overall patient compliance. Lastly, from an economic standpoint, bispecific Ab development is more feasible and acceptable to patients than combination therapy. Therefore, the development of bispecific Abs holds considerable value for future research in AD treatment.

In conclusion, we successfully created a novel treatment modality for AD with a bispecific Ab with stable structure, binding to IL4Rα and IL31Rα, blocking both IL4/IL13-IL4Rα and IL31-IL31Rα signaling pathways, reducing the serum levels of IgE and IL31 (Fig. 6), improving the symptoms of AD in DNFB-induced murine AD model, providing a better opportunity to effectively treat AD.

ABBREVIATIONS

AD, atopic dermatitis; VH, variable heavy chain; VL, variable light chain; scFv, single-chain fragment variable; IgE, immunoglobulin E; SEC, size exclusion chromatography; nrCE-SDS, CE-SDS under nonreducing condition.

SUPPLEMENTARY DATA

Supplementary data are available at *ABT* Online.

ACKNOWLEDGEMENTS

We thank Shenzhen Institute for Drug Control for assistance, Huiming Li, Chen Xu and other members of our laboratory for critical proofreading of the manuscript.

FUNDING

This research was supported by a grant (0592022072200000809) from the Shenzhen Government, China. This research was also funded by Shenzhen Kexing BioPharma Co., Ltd.

CONFLICT OF INTEREST STATEMENT

Feiyan Deng, Yuxin Qiu, Xiangling Zhang, Nining Guo, Junhong Hu, Wenjie Yang, Wei Shang and Suofu Qin are employees in Shenzhen Kexing BioPharma Co., Ltd. Bicheng Liu is the professor of Southeast University School of Medicine.

AUTHOR CONTRIBUTIONS

Suofu Qin (project administrator and supervisor, conceptualized the study), Feiyan Deng (designed the study, acquired the experimental data, performed the statistical analysis, and drafted the manuscript), Yuxin Qiu (designed Abs, acquired the experimental data, and performed the statistical analysis), Xiangling Zhang (acquired the experimental data, and performed the statistical analysis), Nining Guo (designed the study), Junhong Hu (expressed the Abs), Wenjie Yang (acquired the experimental data, and performed the statistical analysis), Wei Shang (edited the manuscript), Bicheng Liu (edited the manuscript), All authors (read and approved the final manuscript)

DATA AVAILABILITY STATEMENT

The data will be available from the corresponding author upon reasonable request.

ETHICS AND CONSENT STATEMENT

Not applicable.

ANIMAL RESEARCH STATEMENT

The animal study protocol was approved by the Institutional Review Board of Shenzhen Institute for Drug Control.

REFERENCES

1. Raimondo, A, Lembo, S. Atopic dermatitis: epidemiology and clinical phenotypes. *Dermatol Pract Concept* 2021; **11**: e2021146.
2. Langan, SM, Irvine, AD, Weidinger, S. Atopic dermatitis. *Lancet* 2020; **396**: 345–60.
3. Li, H, Zhang, Z, Zhang, H *et al.* Update on the pathogenesis and therapy of atopic dermatitis. *Clin Rev Allergy Immunol* 2021; **61**: 324–38.
4. Brandt, B, E. Th2 cytokines and atopic dermatitis. *J Clin Cell Immunol* 2011; **2**:110.
5. Hadi, HA, Tarmizi, AI, Khalid, KA *et al.* The epidemiology and global burden of atopic dermatitis: a narrative review. *Life* 2021; **11**: 936.
6. Novak, N. An update on the role of human dendritic cells in patients with atopic dermatitis. *J Allergy Clin Immunol* 2012; **129**: 879–86.
7. Wollenberg, A, Thomsen, SF, Lacour, JP *et al.* Targeting immunoglobulin E in atopic dermatitis: a review of the existing evidence. *World Allergy Organ J* 2021; **14**: 100519.
8. Howell, MD, Fairchild, HR, Kim, BE *et al.* Th2 cytokines act on S100/A11 to downregulate keratinocyte differentiation. *J Invest Dermatol* 2008; **128**: 2248–58.
9. Furue, M, Chiba, T, Tsuji, G *et al.* Atopic dermatitis: immune deviation, barrier dysfunction, IgE autoreactivity and new therapies. *Allergol Int* 2017; **66**: 398–403.
10. Simpson, EL, Bieber, T, Guttman-Yassky, E *et al.* Two phase 3 trials of dupilumab versus placebo in atopic dermatitis. *N Engl J Med* 2016; **375**: 2335–48.
11. de Bruin-Weller, M, Thaçi, D, Smith, CH *et al.* Dupilumab with concomitant topical corticosteroid treatment in adults with atopic dermatitis with an inadequate response or intolerance to ciclosporin a or when this treatment is medically inadvisable: a placebo-controlled, randomized phase III clinical trial (LIBERTY AD CAFÉ). *Br J Dermatol* 2018; **178**: 1083–101.
12. Blauvelt, A, de Bruin-Weller, M, Gooderham, M *et al.* Long-term management of moderate-to-severe atopic dermatitis with dupilumab and concomitant topical corticosteroids (LIBERTY AD CHRONOS): a 1-year, randomised, double-blinded, placebo-controlled, phase 3 trial. *Lancet* 2017; **389**: 2287–303.
13. Duggan, S. Tralokinumab: first approval. *Drugs* 2021; **81**: 1657–63.
14. Blauvelt, A, Gooderham, M, Bhatia, N *et al.* Tralokinumab efficacy and safety, with or without topical corticosteroids, in north American adults with moderate-to-severe atopic dermatitis: a subanalysis of phase 3 trials ECZTRA 1, 2, and 3. *Dermatol Ther* 2022; **12**: 2499–516.
15. Blauvelt, A, Langley, RG, Lacour, JP *et al.* Long-term 2-year safety and efficacy of tralokinumab in adults with moderate-to-severe atopic dermatitis: interim analysis of the ECZTEND open-label extension trial. *J Am Acad Dermatol* 2022; **87**: 815–24.
16. Keam, SJ. Nemolizumab: first approval. *Drugs* 2022; **82**: 1143–50.
17. Ruzicka, T, Hanifin, JM, Furue, M *et al.* Anti-interleukin-31 receptor a antibody for atopic dermatitis. *N Engl J Med* 2017; **376**: 826–35.
18. Kabashima, K, Matsumura, T, Komazaki, H *et al.* Trial of nemolizumab and topical agents for atopic dermatitis with pruritus. *N Engl J Med* 2020; **383**: 141–50.
19. Labrijn, AF, Janmaat, ML, Reichert, JM *et al.* Bispecific antibodies: a mechanistic review of the pipeline. *Nat Rev Drug Discov* 2019; **18**: 585–608.
20. Brinkmann, U, Kontermann, RE. The making of bispecific antibodies. *MAbs* 2017; **9**: 182–212.
21. Heiss, MM, Murawa, P, Koralewski, P *et al.* The trifunctional antibody catumaxomab for the treatment of malignant ascites due to epithelial cancer: results of a prospective randomized phase II/III trial. *Int J Cancer* 2010; **127**: 2209–21.
22. Burt, R, Warcel, D, Fielding, AK. Blinatumomab, a bispecific B-cell and T-cell engaging antibody, in the treatment of B-cell malignancies. *Hum Vaccin Immunother* 2019; **15**: 594–602.
23. Oldenburg, J, Mahlangu, JN, Kim, B *et al.* Emicizumab prophylaxis in hemophilia a with inhibitors. *N Engl J Med* 2017; **377**: 809–18.
24. Coloma, MJ, Morrison, SL. Design and production of novel tetravalent bispecific antibodies. *Nat Biotechnol* 1997; **15**: 159–63.
25. Pei, M, Wang, Y, Tang, L *et al.* Dual-target bridging ELISA for bispecific antibodies. *Bio Protoc* 2022; **12**:e4522.
26. Weidinger, S, Beck, LA, Bieber, T *et al.* Atopic dermatitis. *Nat Rev Dis Primers* 2018; **4**: 1.
27. Dada, OO, Rao, R, Jones, N *et al.* Comparison of SEC and CE-SDS methods for monitoring hinge fragmentation in IgG1 monoclonal antibodies. *J Pharm Biomed Anal* 2017; **145**: 91–7.
28. Reiter, Y, Brinkmann, U, Kreitman, RJ *et al.* Stabilization of the Fv fragments in recombinant immunotoxins by disulfide bonds engineered into conserved framework regions. *Biochemistry* 1994; **33**: 5451–9.
29. Reiter, Y, Brinkmann, U, Webber, KO *et al.* Engineering interchain disulfide bonds into conserved framework regions of Fv fragments: improved biochemical characteristics of recombinant immunotoxins containing disulfide-stabilized Fv. *Protein Eng* 1994; **7**: 697–704.
30. Metz, S, Haas, AK, Daub, K *et al.* Bispecific digoxigenin-binding antibodies for targeted payload delivery. *Proc Natl Acad Sci U S A* 2011; **108**: 8194–9.
31. Croasdale, R, Wartha, K, Schanzer, JM *et al.* Development of tetravalent IgG1 dual targeting IGF-1R-EGFR antibodies with potent tumor inhibition. *Arch Biochem Biophys* 2012; **526**: 206–18.
32. Schanzer, J, Jekle, A, Nezu, J *et al.* Development of tetravalent, bispecific CCR5 antibodies with antiviral activity against CCR5 monoclonal antibody-resistant HIV-1 strains. *Antimicrob Agents Chemother* 2011; **55**: 2369–78.
33. Scheuer, W, Thomas, M, Hanke, P *et al.* Anti-tumoral, anti-angiogenic and anti-metastatic efficacy of a tetravalent bispecific antibody (TAvi6) targeting VEGF-A and angiopoietin-2. *MAbs* 2016; **8**: 562–73.
34. Liu, FT, Goodarzi, H, Chen, HY. IgE, mast cells, and eosinophils in atopic dermatitis. *Clin Rev Allergy Immunol* 2011; **41**: 298–310.
35. Geha, RS, Jabara, HH, Brodeur, SR. The regulation of immunoglobulin E class-switch recombination. *Nat Rev Immunol* 2003; **3**: 721–32.
36. Munitz, A, Brandt, EB, Mingler, M *et al.* Distinct roles for IL-13 and IL-4 via IL-13 receptor alpha1 and the type II IL-4 receptor in asthma pathogenesis. *Proc Natl Acad Sci U S A* 2008; **105**: 7240–5.
37. Li, C, Maillet, I, Mackowiak, C *et al.* Experimental atopic dermatitis depends on IL-33R signaling via MyD88 in dendritic cells. *Cell Death Dis* 2017; **8**: e2735.
38. Datsi, A, Steinhoff, M, Ahmad, F *et al.* Interleukin-31: the "itchy" cytokine in inflammation and therapy. *Allergy* 2021; **76**: 2982–97.
39. Feld, M, Garcia, R, Buddenkotte, J *et al.* The pruritus- and TH2-associated cytokine IL-31 promotes growth of sensory nerves. *J Allergy Clin Immunol* 2016; **138**: 500–508.e24.
40. Stott, B, Lavender, P, Lehmann, S *et al.* Human IL-31 is induced by IL-4 and promotes TH2-driven inflammation. *J Allergy Clin Immunol* 2013; **132**: 446–454.e5.
41. Neis, MM, Peters, B, Dreuw, A *et al.* Enhanced expression levels of IL-31 correlate with IL-4 and IL-13 in atopic and allergic contact dermatitis. *J Allergy Clin Immunol* 2006; **118**: 930–7.